Engineering 6 (2020) 560–568

Contents lists available at ScienceDirect

Engineering

journal homepage: www.elsevier.com/locate/eng

Research
Green Plant Protection Innovation—Article

Synthesis, Characterization, and Antifungal Evaluation of Thiolactomycin Derivatives

Pei Lv [a,#], Yiliang Chen [a,#], Dawei Wang [b], Xiangwei Wu [a], Qing X. Li [b,c], Rimao Hua [a,*]

[a] Key Laboratory of Agri-Food Safety of Anhui Province, School of Resource and Environment, Anhui Agricultural University, Hefei, 230036, China
[b] State Key Laboratory of Elemento-Organic Chemistry, College of Chemistry, Nankai University, Tianjin 300071, China
[c] Department of Molecular Biosciences and Bioengineering, University of Hawaii at Manoa, Honolulu, HI 96822, USA

ARTICLE INFO

Article history:
Received 23 December 2018
Revised 20 July 2019
Accepted 8 October 2019
Available online 1 April 2020

Keywords:
3-Acylthiotetronic acid
Fungicide
Quantitative structure–activity relationship
Antifungal activity

ABSTRACT

5-Substituted benzylidene 3-acylthiotetronic acids are antifungal. A series of 3-acylthiotetronic acid derivatives with varying substitutions at the 5-position were designed, synthesized, and characterized, based on the binding pose of 3-acyl thiolactone with the protein C171Q KasA. Fungicidal activities of these compounds were screened against *Valsa Mali, Curvularia lunata, Fusarium graminearum*, and *Fusarium oxysporum* f. sp. *lycopersici*. Most target compounds exhibited excellent fungicidal activities against target fungi at the concentration of 50 μg·mL^{-1}. Compounds **11c** and **11i** displayed the highest activity with a broad spectrum. The median effective concentration (EC_{50}) values of **11c** and **11i** were 1.9–10.7 and 3.1–7.8 μg·mL^{-1}, respectively, against the tested fungi, while the EC_{50} values of the fungicides azoxystrobin, carbendazim, and fluopyram were respectively 0.30, 4.22, and > 50 μg·mL^{-1} against *V. Mali*; 6.7, 41.7, and 0.18 μg·mL^{-1} against *C. lunata*; 22.4, 0.42, and 0.43 μg·mL^{-1} against *F. graminearum*; and 4.3, 0.12, and > 50 μg·mL^{-1} against *F. oxysporum* f. sp. *lycopersici*. The structures and activities of the target compounds against *C. lunata* were analyzed to obtain a statistically significant comparative molecular field analysis (CoMFA) model with high prediction abilities (q^2 = 0.9816, r^2 = 0.8060), and its reliability was verified. The different substituents on the benzylidene at the 5-position had significant effects on the activity, while the introduction of a halogen atom at the benzene ring of benzylidene was able to improve the activity against the tested fungi.

1. Introduction

Fungal diseases are increasingly recognized as a worldwide threat to food security, the devastation of agricultural crops, and altered forest ecosystem dynamics [1–3]. To guard against fungal pathogens, a large number of synthetic fungicides that are both economical and efficient have been provided for crop protection since the 1960s, and have played an indispensable role in meeting the soaring food demand due to rapid population growth. However, as a result of the repeated use of fungicides with identical or similar modes of action, a rapid increase in fungicide resistance has appeared, leading to the failure of fungal disease control in crops [4,5]. Meanwhile, non-target and environmental hazards have emerged along with fungicide utilization [6,7]. Therefore, there is a continuing need to develop newer fungicides for fungal disease control in crops.

Fatty acids are essential to fungal survival and are one of the most abundant components of the cell wall in fungi; they function as an ample supply of lipids for membrane biosynthesis, which involves regulating substrates between active sites and increasing local concentrations of intermediates [8–10]. There are two distinct fatty acid biosynthetic pathways of long-chain C_{60-90} α-alkyl-β-hydroxy fatty acids (mycolic acids) [11]. Most bacteria, fungi, and plants possess a fatty acid synthase (FAS) type-II system with dissociated enzymes encoded by separate genes, whereas in mammals, the process of fatty acid synthesis is carried out by a highly integrated FAS type-I multienzyme system that differs significantly from the FAS II enzyme complex [12]. Therefore, FAS II enzymes are an attractive target for the development of new anti-mycobacterial and antimalarial drugs.

Thiolactomycin (TLM), a thiolactone antibiotic, is a known inhibitor of dissociable FAS II enzymes through the inhibition of β-ketoacyl-acyl carrier protein (ACP) synthases (Kases) [13,14]. In

* Corresponding author.
E-mail address: rimaohua@ahau.edu.cn (R. Hua).
# These authors contributed equally to this work.

https://doi.org/10.1016/j.eng.2019.10.016

recent years, many compounds containing a moiety of thiolactone have been found to exhibit noticeable biological activity against many pathogenic bacteria and mycobacteria [15,16]. It has also been found that TLM and its derivatives show antimalarial activity [17,18] and anti-tuberculosis activity [19]. In addition, we have previously demonstrated that 3-acyl thiolactone acts as a potent anti-phytopathogen agent by inhibiting FAS activity [20]. As shown in Fig. 1, the chemical structure that provides the three hydrogen bonds and the hydrophobic tail interacting with the specific amino acid residues in the Kas is crucial for inhibitory potency.

In view of such molecular interactions, it is worth developing new 3-acyl thiolactone derivatives by modifying the substituents of thiolactone for screening highly effective fungicides. Hence, 28 new 3-acylthiotetronic acid derivatives with different substituents of benzylidene at the 5-position were designed and synthesized (See Supplementary data Fig. S1 for compounds **1**–**12a**); these derivatives were expected to exhibit fungicidal activity due to the binding pose of 3-acyl thiolactone with the protein C171Q KasA (Fig. 1) and the proven active group of thiolactone [13–20]. In addition, the comparative molecular field analysis (CoMFA) method implemented in the SYBYL software packages was used to develop predictive three-dimensional (3D) quantitative structure–activity relationship (QSAR) models [21]. This study also predicted the substituents of new thiotetronic acid derivatives with potential antifungal activities based on 3D-QSAR analysis.

2. Materials and methods

2.1. General information

All anhydrous solvents were dried and purified by standard techniques before use. ^{1}H nuclear magnetic resonance (NMR) and ^{13}C NMR spectra were acquired on an Agilent DD2 NMR spectrometer (600 MHz, Agilent Technologies, Inc., USA) at 25 °C with tetramethylsilane as internal standards. Chemical shifts were measured relative to the residual solvent line as an internal standard in ppm (δ). When peak multiplicities are reported, the following abbreviations are used: singlet (s), doublet (d), doublet of doublets (dd), triplet (t), multiplet (m), quarter (q). High-resolution mass spectrometry (HR-MS) data were determined using a Varian quaternion Fourier transform (QFT)–electrospray ionization (ESI) instrument. The melting points (m.p.) of the products were taken on an XT4 MP apparatus (Taike Corp., China) and the thermometer was not corrected. Analytical thin-layer chromatography (TLC) was performed on silica gel GF 254. Column chromatographic purification was performed using silica gel.

2.2. Synthesis

2.2.1. General procedure for the synthesis of compounds ***6a–6i***

4-Hydroxybenzaldehyde (0.5 g, 0.0041 mol), acids (0.0045 mol), and 4-dimethylaminopyridine (DMAP; 0.5 g, 0.0041 mol) were dissolved in dichloromethane (30 mL) at 0 °C. To this solution, 1-ethyl-3-(3-dimethylaminopropyl)carbodiimide (EDC; 1.2 g, 0.0062 mol) in dichloromethane (10 mL) was added dropwise. The mixture was then stirred at room temperature for 12 h, detected by TLC. Upon completion of the reaction, the dichloromethane was removed by rotary evaporation. The crude product was dissolved with ethyl acetate, washed with saturated aqueous $NaHCO_3$ and H_2O, dried over $MgSO_4$, filtered, and then concentrated. The residue was purified by silica gel column chromatography (petroleum ether/ethyl acetate (PE/EA) = 8:1) to obtain **6a**–**6i**:

- **4-Formylphenyl acetate (6a).** Colorless oil; yield 80.4%; ^{1}H NMR (600 MHz, $CDCl_3$) δ: 9.98 (s, 1H), 7.93–7.89 (m, 2H), 7.26 (t, coupling constant J = 5.9 Hz, 2H), and 2.32 (s, 3H). ^{13}C NMR (150 MHz, $CDCl_3$) δ: 190.89, 168.68, 155.30, 133.96, 131.19, 122.35, and 21.14; HR-MS (ESI): mass-to-charge ratio (m/z) calculated for $C_9H_8O_3$ ($[M+H]^+$): 165.0552; found: 165.0554.
- **4-Formylphenyl propionate (6b).** Colorless oil; yield 85.6%; ^{1}H NMR (600 MHz, $CDCl_3$) δ: 9.97 (s, 1H), 7.90 (d, J = 8.5 Hz, 2H), 7.26 (d, J = 8.6 Hz, 2H), 2.61 (q, J = 7.5 Hz, 2H), and 1.26 (t, J = 7.5 Hz, 3H). ^{13}C NMR (150 MHz, $CDCl_3$) δ: 190.92, 172.22, 155.46, 133.87, 131.17, 122.32, 27.75, and 8.92; HR-MS (ESI): m/z calculated for $C_{10}H_{10}O_3$ ($[M+H]^+$): 179.0708; found: 179.0710.
- **4-Formylphenyl hexanoate (6c).** Colorless oil; yield 83.4%; ^{1}H NMR (600 MHz, $CDCl_3$) δ: 9.97 (s, 1H), 7.90 (d, J = 8.4 Hz, 2H), 7.26 (d, J = 8.3 Hz, 2H), 2.57 (t, J = 7.5 Hz, 2H), 1.81–1.62 (m, 2H), 1.46–1.21 (m, 4H), and 0.92 (t, J = 6.8 Hz, 3H). ^{13}C NMR (150 MHz, $CDCl_3$) δ: 190.84, 171.52, 155.48, 133.89, 131.13, 122.32, 34.32, 31.18, 24.46, 22.25, and 13.85; HR-MS (ESI): m/z calculated for $C_{13}H_{16}O_3$ ($[M+H]^+$): 221.1178; found: 221.1180.
- **4-Formylphenyl 4-fluorobenzoate (6d).** White solid; yield 85.4%; m.p. 99–100 °C; ^{1}H NMR (600 MHz, $CDCl_3$) δ: 10.02 (s, 1H), 8.28–8.17 (m, 2H), 7.97 (d, J = 8.0 Hz, 2H), 7.40 (d, J = 8.1 Hz, 2H), and 7.19 (t, J = 8.3 Hz, 2H). ^{13}C NMR (150 MHz, $CDCl_3$) δ: 190.82, 167.21, 165.51, 163.47, 155.49, 134.14, 132.91, 131.24, 125.15, 122.45, 116.03, and 115.88; HR-MS (ESI): m/z calculated for $C_{14}H_9FO_3$ ($[M+H]^+$): 245.0614; found: 245.0618.
- **4-Formylphenyl 4-chlorobenzoate (6e).** White solid; yield 86.7%; m.p. 111–112 °C; ^{1}H NMR (600 MHz, $CDCl_3$) δ: 10.02 (s, 1H), 8.13 (d, J = 8.6 Hz, 2H), 7.97 (d, J = 8.5 Hz, 2H), 7.50 (d, J = 8.5 Hz, 2H), and 7.40 (d, J = 8.5 Hz, 2H). ^{13}C NMR (150 MHz, $CDCl_3$) δ: 190.83, 163.63, 155.40, 140.62, 134.17, 131.61, 131.27, 129.10, 127.33, and 122.43; HR-MS (ESI): m/z calculated for $C_{14}H_9ClO_3$ ($[M+H]^+$): 261.0318; found: 261.0322.

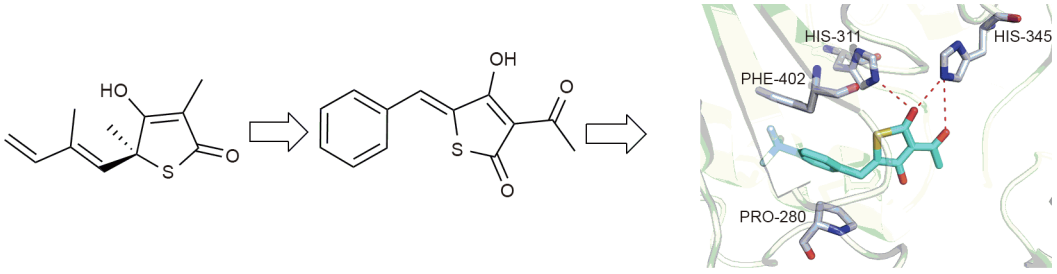

Fig. 1. TLM (left), 3-acetyl thiotetronic acid lead (middle), and predicted docking pose (right) of 3-acetyl thiotetronic acid in a complex with C171Q KasA enzyme (protein data bank (PDB): 4c6u).

• **4-Formylphenyl 4-bromobenzoate (6f).** White solid; yield 91.5%; m.p. 112–113 °C; ^{1}H NMR (600 MHz, $CDCl_3$) δ: 10.02 (s, 1H), 8.05 (d, J = 8.5 Hz, 2H), 7.97 (d, J = 8.5 Hz, 2H), 7.67 (d, J = 8.5 Hz, 2H), and 7.40 (d, J = 8.5 Hz, 2H). ^{13}C NMR (150 MHz, $CDCl_3$) δ: 190.81, 163.78, 155.39, 134.18, 132.10, 131.68, 131.26, 129.34, 127.80, and 122.42; HR-MS (ESI): m/z calculated for $C_{14}H_9BrO_3$ ($[M+H]^+$): 304.9813; found: 304.9814.

• **4-Formylphenyl 4-methylbenzoate (6g).** White solid; yield 86.9%; m.p. 112–113 °C; ^{1}H NMR (600 MHz, $CDCl_3$) δ: 10.01 (s, 1H), 8.08 (d, J = 8.2 Hz, 2H), 7.96 (d, J = 8.6 Hz, 2H), 7.40 (d, J = 8.5 Hz, 2H), 7.32 (d, J = 7.9 Hz, 2H), and 2.46 (s, 3H). ^{13}C NMR (150 MHz, $CDCl_3$) δ: 190.97, 164.53, 155.78, 144.97, 133.95, 131.23, 130.30, 129.42, 126.10, 122.56, and 21.79; HR-MS (ESI): m/z calculated for $C_{15}H_{12}O_3$ ($[M+H]^+$): 241.0865; found: 241.0868.

• **4-Formylphenyl 4-(trifluoromethyl)benzoate (6h).** White solid; yield 79.8%; m.p. 85–86 °C; ^{1}H NMR (600 MHz, $CDCl_3$) δ: 10.03 (s, 1H), 8.32 (d, J = 8.1 Hz, 2H), 7.99 (d, J = 8.5 Hz, 2H), 7.80 (d, J = 8.2 Hz, 2H), and 7.42 (d, J = 8.4 Hz, 2H). ^{13}C NMR (150 MHz, $CDCl_3$) δ: 190.83, 163.32, 155.21, 135.50, 135.29, 134.31, 132.13, 131.33, 131.11, 130.66, 125.75, 124.34, 122.53, and 122.34; HR-MS (ESI): m/z calculated for $C_{15}H_9F_3O_3$ ($[M+H]^+$): 295.0582; found: 295.0587.

• **4-Formylphenyl 4-methoxybenzoate (6i).** White solid; yield 89.8%; m.p. 95–96 °C; ^{1}H NMR (600 MHz, $CDCl_3$) δ: 10.01 (s, 1H), 8.14 (d, J = 8.7 Hz, 2H), 7.95 (d, J = 8.4 Hz, 2H), 7.39 (d, J = 8.3 Hz, 2H), 6.99 (d, J = 8.7 Hz, 2H), and 3.89 (s, 3H). ^{13}C NMR (150 MHz, $CDCl_3$) δ: 190.95, 164.18, 155.85, 133.89, 132.42, 131.20, 122.57, 121.10, 113.97, and 55.54; HR-MS (ESI): m/z calculated for $C_{15}H_{12}O_4$ ($[M+H]^+$): 257.0814; found: 257.0816.

*2.2.2. General procedure for the preparation of compounds **8a–8g***

4-Formylbenzoic acid (0.5 g, 0.0033 mol), alcohols (0.0030 mol), and DMAP (0.4 g, 0.0033 mol) were dissolved in dichloromethane (30 mL) at 0 °C. To this solution, EDC (1.0 g, 0.0050 mol) in dichloromethane (10 mL) was added dropwise. The mixture was then stirred at room temperature for 12 h, detected by TLC. Upon completion of the reaction, dichloromethane was removed by rotary evaporation. The crude product was dissolved with ethyl acetate, washed with saturated aqueous $NaHCO_3$ and H_2O, dried over $MgSO_4$, filtered, and then concentrated. The residue was purified by silica gel column chromatography (PE/EA = 15:1) to obtain **8a–8g**:

• **Methyl 4-formylbenzoate (8a).** White solid; yield 91.1%; m.p. 58–59 °C; ^{1}H NMR (600 MHz, $CDCl_3$) δ: 10.08 (s, 1H), 8.18 (d, J = 8.2 Hz, 2H), 7.93 (d, J = 8.1 Hz, 2H), and 3.94 (s, 3H). ^{13}C NMR (150 MHz, $CDCl_3$) δ: 191.61, 166.02, 139.09, 135.04, 130.15, 129.48, and 52.55; HR-MS (ESI) m/z calculated for $C_9H_8O_3$ ($[M+H]^+$): 165.0552; found: 165.0551.

• **Ethyl 4-formylbenzoate (8b).** Colorless oil; yield 81.9%; ^{1}H NMR (600 MHz, $CDCl_3$) δ: 10.08 (s, 1H), 8.20–8.10 (m, 2H), 7.93 (d, J = 8.2 Hz, 2H), 4.40 (q, J = 7.1 Hz, 2H), and 1.40 (t, J = 7.2 Hz, 3H). ^{13}C NMR (150 MHz, $CDCl_3$) δ: 191.69, 165.55, 139.02, 135.41, 130.08, 129.50, 61.59, and 14.23; HR-MS (ESI) m/z calculated for $C_{10}H_{10}O_3$ ($[M+H]^+$): 179.0708; found: 179.0709.

• **Isopropyl 4-formylbenzoate (8c).** Colorless oil; yield 83.7%; ^{1}H NMR (600 MHz, $CDCl_3$) δ: 10.08 (s, 1H), 8.16 (d, J = 8.2 Hz, 2H), 7.92 (d, J = 8.4 Hz, 2H), 5.29–5.22 (m, 1H), and 1.37 (d, J = 6.3 Hz, 6H). ^{13}C NMR (150 MHz, $CDCl_3$) δ: 191.65, 165.00, 138.97, 135.85, 130.02, 129.39, 69.19, and 21.84; HR-MS (ESI) m/z calculated for $C_{11}H_{12}O_3$ ($[M+H]^+$): 193.0865; found: 193.0868.

• **Propyl 4-formylbenzoate (8d).** Colorless oil; yield 83.1%; ^{1}H NMR (600 MHz, $CDCl_3$) δ: 10.09 (s, 1H), 8.20–8.11 (m, 2H), 7.94 (d, J = 8.3 Hz, 2H), 4.31 (t, J = 6.7 Hz, 2H), 1.83–1.76 (m, 2H), and 1.03 (t, J = 7.4 Hz, 3H). ^{13}C NMR (150 MHz, $CDCl_3$) δ: 191.68, 165.60, 139.03, 135.45, 130.11, 129.47, 67.14, 22.01, and 10.46; HR-MS (ESI) m/z calculated for $C_{11}H_{12}O_3$ ($[M+H]^+$): 193.0865; found: 193.0868.

• **Butyl 4-formylbenzoate (8e).** Colorless oil; yield 89.4%; ^{1}H NMR (600 MHz, $CDCl_3$) δ: 10.08 (s, 1H), 8.17 (d, J = 8.2 Hz, 2H), 7.93 (d, J = 8.1 Hz, 2H), 4.34 (t, J = 6.6 Hz, 2H), 1.79–1.72 (m, 2H), 1.51–1.43 (m, 2H), and 0.97 (t, J = 7.4 Hz, 3H). ^{13}C NMR (150 MHz, $CDCl_3$) δ: 191.67, 165.60, 139.02, 135.44, 130.10, 129.46, 65.45, 30.65, 19.21, and 13.71; HR-MS (ESI) m/z calculated for $C_{12}H_{14}O_3$ ($[M+H]^+$): 207.1021; found: 207.1022.

• **Octyl 4-formylbenzoate (8f).** Colorless oil; yield 79.6%; ^{1}H NMR (600 MHz, $CDCl_3$) δ: 10.09 (s, 1H), 8.18 (d, J = 8.2 Hz, 2H), 7.94 (d, J = 8.3 Hz, 2H), 4.34 (t, J = 6.7 Hz, 2H), 1.81–1.72 (m, 2H), 1.50–1.20 (m, 10H), and 0.87 (t, J = 6.6 Hz, 3H). ^{13}C NMR (150 MHz, $CDCl_3$) δ: 191.58, 165.58, 139.06, 135.49, 130.10, 129.44, 65.75, 31.74, 29.16, 28.62, 25.97, 22.59, and 14.03; HR-MS (ESI): m/z calculated for $C_{16}H_{22}O_3$ ($[M+H]^+$): 263.1647; found: 263.1650.

• **Benzyl 4-formylbenzoate (8g).** White solid; yield 73.8%; m.p. 43–44 °C; ^{1}H NMR (600 MHz, $CDCl_3$) δ: 10.09 (s, 1H), 8.22 (d, J = 8.1 Hz, 2H), 7.94 (d, J = 8.1 Hz, 2H), 7.45 (d, J = 7.3 Hz, 2H), 7.40 (t, J = 7.4 Hz, 2H), 7.36 (t, J = 7.2 Hz, 1H), 5.39 (s, 2H). ^{13}C NMR (150 MHz, $CDCl_3$) δ: 191.60, 165.37, 139.18, 135.51, 135.06, 130.29, 129.50, 128.68, 128.49, 128.33, and 67.30; HR-MS (ESI) m/z calculated for $C_{15}H_{12}O_3$ ($[M+H]^+$): 241.0865; found: 241.0866.

*2.2.3. General procedure for compounds **9a–9i**, **10a–10g**, **11a–11m**, and **12a***

A solution of 158 mg (1 mmol) of 3-acetylthiophene-2,4 (3*H*,5*H*)-dione (**4**) and appropriate substituted aromatic aldehyde (1.1 mmol) in 50 mL of toluene containing *p*-TsOH (30 mg, 0.17 mmol) was refluxed with the azeotropic removal of water and detected by TLC. The mixture was cooled to room temperature, and the precipitate 5-substuted benzylidene 3-acylthiotetronic acid (i.e., **9a–9i, 10a–10g, 11a–11m**, and **12a**) was filtered off and recrystallized from the MeOH-ethyl acetate:

• **4-((4-Acetyl-3-hydroxy-5-oxothiophen-2(5*H*)-ylidene) methyl)phenyl acetate (9a).** Yellow solid; yield 70.9%; m.p. 192–193 °C; ^{1}H NMR (600 MHz, $CDCl_3$) δ: 7.81 (s, 1H), 7.61 (d, J = 8.6 Hz, 2H), 7.21 (d, J = 8.6 Hz, 2H), 2.61 (s, 3H), 2.32 (s, 3H). ^{13}C NMR (150 MHz, $CDCl_3$) δ: 197.57, 187.14, 168.94, 152.17, 133.50, 132.31, 131.62, 131.29, 126.07, 122.45, 116.34, 108.59, 25.69, and 21.15; HR-MS (ESI) m/z calculated for $C_{15}H_{12}O_5S$ ($[M+H]^+$): 305.0484; found: 305.0485.

• **4-((4-Acetyl-3-hydroxy-5-oxothiophen-2(5*H*)-ylidene) methyl)phenyl propionate (9b).** Yellow solid; yield 65.7%; m.p. 167–168 °C; ^{1}H NMR (600 MHz, $CDCl_3$) δ: 7.80 (s, 1H), 7.61 (d, J = 8.6 Hz, 2H), 7.21 (d, J = 8.6 Hz, 2H), 2.64–2.58 (m, 5H), and 1.26 (q, J = 7.7 Hz, 3H). ^{13}C NMR (150 MHz, $CDCl_3$) δ: 197.58, 187.14, 172.46, 152.33, 132.31, 131.70, 131.16, 125.95, 122.43, 108.59, 27.76, 25.70, and 8.96; HR-MS (ESI) m/z calculated for $C_{16}H_{14}O_5S$ ($[M+H]^+$): 319.0640; found: 319.0642.

• **4-((4-Acetyl-3-hydroxy-5-oxothiophen-2(5*H*)-ylidene) methyl)phenyl hexanoate (9c).** Yellow solid; yield 66.8%; m.p. 124–125 °C; ^{1}H NMR (600 MHz, $CDCl_3$) δ: 7.81 (s, 1H), 7.61 (d, J = 8.5 Hz, 2H), 7.20 (d, J = 8.5 Hz, 2H), 2.61 (s, 3H), 2.57 (t, J = 7.5 Hz, 2H), 1.81–1.71 (m, 2H), 1.39 (d, J = 3.3 Hz, 4H), and 0.93 (t, J = 6.8 Hz, 3H). ^{13}C NMR (150 MHz, $CDCl_3$) δ: 197.54, 187.12, 171.77, 152.35, 132.28, 131.67, 131.16, 125.98, 122.45, 108.59, 34.34, 31.21, 25.66, 24.51, 22.27, and 13.87; HR-MS (ESI) m/z calculated for $C_{19}H_{20}O_5S$ ($[M+H]^+$): 361.1110; found: 361.1112.

• **4-((4-Acetyl-3-hydroxy-5-oxothiophen-2(5*H*)-ylidene) methyl)phenyl 4-fluorobenzoate (9d).** Yellow solid; yield 65.4%; m.p. 191–192 °C; ^{1}H NMR (600 MHz, $CDCl_3$) δ: 8.22 (dd, J = 8.4, 5.5 Hz, 2H), 7.84 (s, 1H), 7.67 (d, J = 8.4 Hz, 2H), 7.34 (d, J = 8.4 Hz, 2H), 7.20 (t, J = 8.5 Hz, 2H), and 2.62 (s, 3H). ^{13}C NMR (150 MHz, $CDCl_3$) δ: 197.53, 187.12, 167.17, 165.47, 163.69, 152.35, 132.89, 132.36, 131.51, 126.25, 125.28, 122.54, 116.00,

115.85, 108.59, and 25.64; HR-MS (ESI) *m/z* calculated for $C_{20}H_{13}FO_5S$ ($[M+H]^+$): 385.0546; found: 385.0547.

• **4-((4-Acetyl-3-hydroxy-5-oxothiophen-2(5*H*)-ylidene) methyl)phenyl 4-chlorobenzoate (9e).** Yellow solid; yield 69.9%; m.p. 188–189 °C; ^{1}H NMR (600 MHz, $CDCl_3$) δ: 7.83 (s, 1H), 7.66 (d, *J* = 8.4 Hz, 2H), 7.50 (d, *J* = 8.3 Hz, 2H), 7.33 (d, *J* = 8.3 Hz, 2H), and 2.62 (s, 3H). ^{13}C NMR (150 MHz, $CDCl_3$) δ: 197.60, 187.13, 163.86, 152.25, 140.53, 132.41, 131.60, 131.55, 131.51, 129.07, 127.42, 126.23, 122.53, 108.59, and 25.73; HR-MS (ESI) *m/z* calculated for $C_{20}H_{13}ClO_5S$ ($[M+H]^+$): 401.0250; found: 401.0251.

• **4-((4-Acetyl-3-hydroxy-5-oxothiophen-2(5*H*)-ylidene) methyl)phenyl 4-bromobenzoate (9f).** Yellow solid; yield 65.1%; m.p. 184–185 °C; ^{1}H NMR (600 MHz, $CDCl_3$) δ: 8.05 (d, *J* = 8.4 Hz, 2H), 7.84 (s, 1H), 7.67 (d, *J* = 7.9 Hz, 4H), 7.34 (d, *J* = 8.5 Hz, 2H), and 2.62 (s, 3H). ^{13}C NMR (150 MHz, $CDCl_3$) δ: 197.60, 187.14, 164.03, 152.23, 132.41, 132.08, 131.70, 131.54, 129.27, 127.88, 126.25, 122.52, 108.60, and 25.73; HR-MS (ESI) *m/z* calculated for $C_{20}H_{13}BrO_5S$ ($[M+H]^+$): 444.9745; found: 444.9746.

• **4-((4-Acetyl-3-hydroxy-5-oxothiophen-2(5*H*)-ylidene) methyl)phenyl 4-methylbenzoate (9g).** Yellow solid; yield 69.3%; m.p. 181–182 °C; ^{1}H NMR (600 MHz, $CDCl_3$) δ: 8.08 (d, *J* = 8.1 Hz, 2H), 7.85 (s, 1H), 7.67 (d, *J* = 8.6 Hz, 2H), 7.33 (dd, *J* = 15.2, 8.3 Hz, 4H), and 2.62 (s, 3H), and 2.46 (s, 3H). ^{13}C NMR (150 MHz, $CDCl_3$) δ: 197.58, 187.14, 164.72, 152.65, 144.85, 132.36, 131.75, 131.25, 130.28, 129.38, 126.24, 126.01, 122.65, 108.62, 25.71, and 21.78; HR-MS (ESI) *m/z* calculated for $C_{21}H_{16}O_5S$ ($[M+H]^+$): 381.0797; found: 381.0796.

• **4-((4-Acetyl-3-hydroxy-5-oxothiophen-2(5*H*)-ylidene) methyl)phenyl 4-(trifluoromethyl)benzoate (9h).** Yellow solid; yield 67.4%; m.p. 195–196 °C; ^{1}H NMR (600 MHz, $CDCl_3$) δ: 8.32 (d, *J* = 8.2 Hz, 2H), 7.85 (s, 1H), 7.80 (d, *J* = 8.2 Hz, 2H), 7.69 (d, *J* = 8.6 Hz, 2H), 7.36 (d, *J* = 8.6 Hz, 2H), and 2.63 (s, 3H). ^{13}C NMR (150 MHz, $CDCl_3$) δ: 197.53, 187.12, 163.51, 152.07, 132.40, 131.74, 131.38, 130.63, 126.48, 125.70, 122.44, 108.59, and 25.63; HR-MS (ESI) *m/z* calculated for $C_{21}H_{13}F_3O_5S$ ($[M+H]^+$): 435.0514; found: 435.517.

• **4-((4-Acetyl-3-hydroxy-5-oxothiophen-2(5*H*)-ylidene) methyl)phenyl 4-methoxybenzoate (9i).** Yellow solid; yield 63.9%; m.p. 155–156 °C; ^{1}H NMR (600 MHz, $CDCl_3$) δ: 8.14 (d, *J* = 8.2 Hz, 2H), 7.84 (s, 1H), 7.65 (d, *J* = 8.2 Hz, 2H), 7.33 (d, *J* = 8.2 Hz, 2H), 6.99 (d, *J* = 8.3 Hz, 2H), 3.90 (s, 3H), and 2.62 (s, 3H). ^{13}C NMR (150 MHz, $CDCl_3$) δ: 197.64, 187.25, 187.05, 164.39, 164.13, 152.70, 132.40, 131.83, 131.14, 125.88, 122.70, 121.20, 113.93, 108.61, 55.56, and 25.77; HR-MS (ESI) *m/z* calculated for $C_{21}H_{16}O_6S$ ($[M+H]^+$): 397.0746; found: 397.0747.

• **Methyl 4-((4-acetyl-3-hydroxy-5-oxothiophen-2(5*H*)-ylidene)-methyl)benzoate (10a).** Yellow solid; yield 63.6%; m.p. 177–178 °C; ^{1}H NMR (600 MHz, $CDCl_3$) δ: 8.10 (d, *J* = 8.4 Hz, 2H), 7.82 (s, 1H), 7.64 (d, *J* = 8.3 Hz, 2H), 3.94 (s, 3H), and 2.62 (s, 3H). ^{13}C NMR (150 MHz, $CDCl_3$) δ: 197.33, 187.35, 186.81, 166.15, 137.70, 131.25, 130.92, 130.71, 130.14, 128.71, 108.55, 52.40, and 25.46; HR-MS (ESI) *m/z* calculated for $C_{15}H_{12}O_5S$ ($[M+H]^+$): 305.0484; found: 305.0486.

• **Ethyl 4-((4-acetyl-3-hydroxy-5-oxothiophen-2(5*H*)-ylidene)-methyl)benzoate (10b).** Yellow solid; yield 64.5%; m.p. 147–148 °C; ^{1}H NMR (600 MHz, $CDCl_3$) δ: 8.12 (d, *J* = 8.4 Hz, 2H), 7.83 (s, 1H), 7.64 (d, *J* = 8.3 Hz, 2H), 4.39 (q, *J* = 7.1 Hz, 2H), 2.62 (s, 3H), and 1.40 (t, *J* = 7.1 Hz, 3H). ^{13}C NMR (150 MHz, $CDCl_3$) δ: 197.36, 187.33, 186.87, 165.68, 137.59, 131.63, 131.03, 130.68, 130.11, 128.60, 108.57, 61.36, 25.49, and 14.28; HR-MS (ESI) *m/z* calculated for $C_{16}H_{14}O_5S$ ($[M+H]^+$): 319.0640; found: 319.0640.

• **Isopropyl 4-((4-acetyl-3-hydroxy-5-oxothiophen-2(5*H*)-ylidene)methyl)benzoate (10c).** Yellow solid; yield 70.1%; m.p. 157–158 °C; ^{1}H NMR (600 MHz, $CDCl_3$) δ: 8.10 (d, *J* = 8.3 Hz, 2H), 7.83 (s, 1H), 7.63 (d, *J* = 8.2 Hz, 2H), 5.29–5.22 (m, 1H), 2.62 (s, 3H), and 1.37 (d, *J* = 6.3 Hz, 6H). ^{13}C NMR (150 MHz, $CDCl_3$) δ: 197.34, 187.31, 186.86, 165.14, 137.48, 132.08, 131.08, 130.63, 130.07, 128.52, 108.56, 68.89, 25.47, and 21.90; HR-MS (ESI) *m/z* calculated for $C_{17}H_{16}O_5S$ ($[M+H]^+$): 333.0797; found: 333.0800.

• **Propyl 4-((4-acetyl-3-hydroxy-5-oxothiophen-2(5*H*)-ylidene)methyl)benzoate (10d).** Yellow solid; yield 70.6%; m.p. 142–143 °C; ^{1}H NMR (600 MHz, $CDCl_3$) δ: 8.12 (d, *J* = 8.3 Hz, 2H), 7.83 (s, 1H), 7.65 (d, *J* = 8.3 Hz, 2H), 4.30 (t, *J* = 6.7 Hz, 2H), 2.62 (s, 3H), 1.84–1.77 (m, 2H), and 1.03 (t, *J* = 7.4 Hz, 3H). ^{13}C NMR (150 MHz, $CDCl_3$) δ: 197.34, 187.34, 186.84, 165.72, 137.60, 131.67, 131.01, 130.68, 130.10, 128.62, 108.57, 66.91, 25.46, 22.06, and 10.48; HR-MS (ESI) *m/z* calculated for $C_{17}H_{16}O_5S$ ($[M+H]^+$): 333.0797; found: 333.0800.

• **Butyl 4-((4-acetyl-3-hydroxy-5-oxothiophen-2(5*H*)-ylidene)-methyl)benzoate (10e).** Yellow solid; yield 66.7%; m.p. 112–113 °C; ^{1}H NMR (600 MHz, $CDCl_3$) δ: 8.11 (d, *J* = 8.3 Hz, 2H), 7.82 (s, 1H), 7.64 (d, *J* = 8.3 Hz, 2H), 4.34 (t, *J* = 6.6 Hz, 2H), 2.62 (s, 3H), 1.79–1.72 (m, 2H), 1.52–1.43 (m, 2H), and 0.98 (t, *J* = 7.4 Hz, 3H). ^{13}C NMR (150 MHz, $CDCl_3$) δ: 197.34, 187.33, 186.84, 165.72, 137.58, 131.66, 131.01, 130.69, 130.10, 128.60, 108.55, 65.23, 30.70, 25.47, 19.25, and 13.74; HR-MS (ESI) *m/z* calculated for $C_{18}H_{18}O_5S$ ($[M+H]^+$): 347.0953; found: 347.0954.

• **Octyl 4-((4-acetyl-3-hydroxy-5-oxothiophen-2(5*H*)-ylidene)-methyl)benzoate (10f).** Yellow solid; yield 65.4%; m.p. 113–114 °C; ^{1}H NMR (600 MHz, $CDCl_3$) δ: 8.11 (d, *J* = 8.3 Hz, 2H), 7.83 (s, 1H), 7.64 (d, *J* = 8.3 Hz, 2H), 4.33 (t, *J* = 6.7 Hz, 2H), 2.62 (d, *J* = 7.9 Hz, 3H), 1.80–1.73 (m, 2H), 1.47–1.40 (m, 2H), 1.39–1.23 (m, 8H), and 0.88 (t, *J* = 6.8 Hz, 3H). ^{13}C NMR (150 MHz, $CDCl_3$) δ: 197.32, 187.34, 186.82, 165.72, 137.59, 131.69, 131.01, 130.68, 130.10, 128.63, 108.56, 65.54, 31.76, 29.18, 28.67, 26.00, 25.44, 22.61, and 14.06; HR-MS (ESI) *m/z* calculated for $C_{22}H_{26}O_5S$ ($[M+H]^+$): 403.0579; found: 403.1580.

• **Benzyl 4-((4-acetyl-3-hydroxy-5-oxothiophen-2(5*H*)-ylidene)methyl)benzoate (10g).** Yellow solid; yield 69.8%; m.p. 168–169 °C; ^{1}H NMR (600 MHz, $CDCl_3$) δ: 8.14 (d, *J* = 8.4 Hz, 2H), 7.82 (s, 1H), 7.64 (d, *J* = 8.3 Hz, 2H), 7.45 (d, *J* = 7.1 Hz, 2H), 7.40 (t, *J* = 7.3 Hz, 2H), 7.35 (dd, *J* = 8.5, 6.0 Hz, 1H), 5.38 (s, 2H), and 2.62 (s, 3H). ^{13}C NMR (150 MHz, $CDCl_3$) δ: 197.31, 187.35, 186.78, 165.49, 137.82, 135.69, 131.25, 130.89, 130.70, 130.26, 128.79, 128.64, 128.39, 128.25, 108.55, 67.07, and 25.44; HR-MS (ESI) *m/z* calculated for $C_{21}H_{16}O_5S$ ($[M+H]^+$): 381.0797; found: 381.0796.

• **3-Acetyl-5-(2-bromobenzylidene)-4-hydroxythiophen-2 (5*H*)-one (11a).** Yellow solid; yield 66.9%; m.p. 152–153 °C; ^{1}H NMR (600 MHz, $CDCl_3$) δ: 8.14 (s, 1H), 7.66 (dd, *J* = 11.3, 8.5 Hz, 2H), 7.40 (t, *J* = 7.5 Hz, 1H), 7.26–7.24 (m, 1H), and 2.62 (s, 3H). ^{13}C NMR (150 MHz, $CDCl_3$) δ: 197.50, 187.17, 186.97, 133.65, 131.39, 130.25, 128.99, 127.79, 126.69, 108.94, and 25.63; HR-MS (ESI) *m/z* calculated for $C_{13}H_9BrO_3S$ ($[M+H]^+$): 324.9534; found: 324.9555.

• **3-Acetyl-5-(3-bromobenzylidene)-4-hydroxythiophen-2 (5*H*)-one (11b).** Yellow solid; yield 69.7%; m.p. 150–151 °C; ^{1}H NMR (600 MHz, $CDCl_3$) δ: 7.72 (d, *J* = 7.2 Hz, 2H), 7.52 (dd, *J* = 11.8, 8.2 Hz, 2H), 7.33 (t, *J* = 7.9 Hz, 1H), and 2.62 (s, 3H). ^{13}C NMR (150 MHz, $CDCl_3$) δ: 197.32, 187.25, 186.74, 135.66, 133.64, 133.26, 130.56, 129.14, 127.85, 123.20, 108.55, and 25.45; HR-MS (ESI) *m/z* calculated for $C_{13}H_9BrO_3S$ ($[M+H]^+$): 324.9534; found: 324.9555.

• **3-Acetyl-5-(4-bromobenzylidene)-4-hydroxythiophen-2(5*H*)-one (11c).** Yellow solid; yield 78.6%; m.p. 176–177 °C; ^{1}H NMR (600 MHz, $CDCl_3$) δ: 7.74 (s, 1H), 7.59 (d, *J* = 8.1 Hz, 2H), 7.44 (d, *J* = 8.1 Hz, 2H), and 2.61 (s, 3H). ^{13}C NMR (150 MHz, $CDCl_3$) δ: 197.42, 187.18, 186.80, 132.47, 132.22, 131.17, 126.90, 125.28, 108.53, and 25.54; HR-MS (ESI) *m/z* calculated for $C_{13}H_9BrO_3S$ ($[M+H]^+$): 324.9534; found: 324.9555.

• **3-Acetyl-5-(2-fluorobenzylidene)-4-hydroxythiophen-2(5*H*)-one (11d).** Yellow solid; yield 67.5%; m.p. 165–166 °C; ^{1}H NMR

(600 MHz, DMSO-d_6) δ: 7.75 (s, 1H), 7.61 (t, J = 7.2 Hz, 1H), 7.48 (d, J = 6.2 Hz, 1H), 7.39–7.29 (m, 2H), and 2.44 (s, 3H). ^{13}C NMR (150 MHz, DMSO-d_6) δ: 194.31, 186.63, 185.78, 161.98, 160.31, 132.37, 129.74, 125.60, 122.50, 119.47, 116.43, 107.54, and 27.07; HR-MS (ESI) m/z calculated for $C_{13}H_9FO_3S$ ([M+H]$^+$): 265.0335; found: 265.0336.

• **3-Acetyl-5-(3-fluorobenzylidene)-4-hydroxythiophen-2(5*H*)-one (11e).** Yellow solid; yield 63.8%; m.p. 151–152 °C; ^{1}H NMR (600 MHz, DMSO-d_6) δ: 7.75 (s, 1H), 7.53 (dd, J = 14.2, 7.4 Hz, 1H), 7.45 (t, J = 8.9 Hz, 2H), 7.27 (t, J = 8.4 Hz, 1H), and 2.45 (s, 3H). ^{13}C NMR (150 MHz, DMSO-d_6) δ: 195.17, 186.65, 186.02, 163.47, 161.85, 136.73, 131.59, 129.58, 128.67, 126.73, 117.42, 117.27, 117.12, 107.91, and 26.68; HR-MS (ESI) m/z calculated for $C_{13}H_9FO_3S$ ([M+H]$^-$): 265.0335; found: 265.0336.

• **3-Acetyl-5-(2-chlorobenzylidene)-4-hydroxythiophen-2(5*H*)-one (11g).** Yellow solid; yield 64.9%; m.p. 157–158 °C; ^{1}H NMR (600 MHz, $CDCl_3$) δ: 8.20 (s, 1H), 7.68–7.65 (m, 1H), 7.47 (dd, J = 7.3, 1.4 Hz, 1H), 7.38–7.31 (m, 2H), and 2.62 (s, 3H). ^{13}C NMR (150 MHz, $CDCl_3$) δ: 197.49, 187.08, 136.26, 131.97, 131.33, 130.30, 130.13, 128.84, 128.65, 127.19, 108.87, and 25.62; HR-MS (ESI) m/z calculated for $C_{13}H_9ClO_3S$ ([M+H]$^+$): 281.0039; found: 281.0040.

• **3-Acetyl-5-(3-chlorobenzylidene)-4-hydroxythiophen-2(5*H*)-one (11h).** Yellow solid; yield 62.9%; m.p. 142–143 °C; ^{1}H NMR (600 MHz, $CDCl_3$) δ: 7.73 (s, 1H), 7.55 (s, 1H), 7.47 (d, J = 6.7 Hz, 1H), 7.42–7.36 (m, 2H), and 2.62 (s, 3H). ^{13}C NMR (150 MHz, $CDCl_3$) δ: 197.34, 187.26, 186.76, 135.38, 135.17, 130.71, 130.33, 128.77, 127.82, 108.55, and 25.46; HR-MS (ESI) m/z calculated for $C_{13}H_9ClO_3S$ ([M+H]$^+$): 281.0039; found: 281.0040.

• **3-((4-Acetyl-3-hydroxy-5-oxothiophen-2(5*H*)-ylidene) methyl)benzonitrile (11j).** Yellow solid; yield 64.8%; m.p. 171–172 °C; ^{1}H NMR (600 MHz, $CDCl_3$) δ: 7.84 (s, 1H), 7.81 (d, J = 7.9 Hz, 1H), 7.76 (s, 1H), 7.68 (d, J = 7.6 Hz, 1H), 7.59 (t, J = 7.8 Hz, 1H), and 2.63 (s, 3H). ^{13}C NMR (150 MHz, $CDCl_3$) δ: 197.18, 187.47, 186.20, 134.93, 134.27, 133.98, 133.13, 130.00, 129.35, 129.20, 117.87, 113.64, 108.38, and 25.29; HR-MS (ESI) m/z calculated for $C_{14}H_9NO_3S$ ([M+H]$^+$): 272.0381; found: 272.0382.

• **3-Acetyl-4-hydroxy-5-(3-(trifluoromethyl)benzylidene) thiophen-2(5*H*)-one (11k).** Yellow solid; yield 70.8%; m.p. 125–126 °C; ^{1}H NMR (600 MHz, DMSO-d_6) δ: 7.96 (s, 1H), 7.89 (d, J = 6.8 Hz, 1H), 7.79 (s, 1H), 7.72 (dd, J = 16.0, 8.7 Hz, 2H), and 2.43 (s, 3H). ^{13}C NMR (150 MHz, DMSO-d_6) δ: 194.35, 186.41, 186.02, 135.83, 133.93, 131.26, 130.66, 127.24, 127.03, 126.20, 107.45, and 27.18; HR-MS (ESI) m/z calculated for $C_{14}H_9F_3O_3S$ ([M+H]$^+$): 315.0303; found: 315.0305.

• **3-Acetyl-4-hydroxy-5-(3-methoxybenzylidene)thiophen-2 (5*H*)-one (11l).** Yellow solid; yield 67.2%; m.p. 141–143 °C; ^{1}H NMR (600 MHz, $CDCl_3$) δ: 7.79 (s, 1H), 7.37 (t, J = 8.0 Hz, 1H), 7.18 (d, J = 7.6 Hz, 1H), 7.10 (s, 1H), 6.97 (dd, J = 8.2, 1.5 Hz, 1H), 3.85 (s, 3H), and 2.61 (s, 3H). ^{13}C NMR (150 MHz, $CDCl_3$) δ: 197.57, 187.32, 187.07, 159.95, 134.88, 132.76, 130.09, 126.25, 123.83, 116.94, 115.46, 108.68, 55.35, and 25.70; HR-MS (ESI) m/z calculated for $C_{14}H_{12}O_4S$ ([M+H]$^+$): 277.0535; found: 277.0538.

• **3-Acetyl-5-(biphenyl-4-ylmethylene)-4-hydroxythiophen-2(5*H*)-one (11m).** Yellow solid; yield 64.4%; m.p. 123–124 °C; ^{1}H NMR (600 MHz, $CDCl_3$) δ: 7.87 (s, 1H), 7.71 (d, J = 8.4 Hz, 2H), 7.67 (d, J = 8.3 Hz, 2H), 7.63 (d, J = 7.3 Hz, 2H), 7.47 (t, J = 7.6 Hz, 2H), 7.39 (t, J = 7.3 Hz, 1H), and 2.62 (s, 3H). ^{13}C NMR (150 MHz, $CDCl_3$) δ: 197.67, 187.35, 186.96, 143.32, 139.64, 132.48, 131.69, 128.98, 128.20, 127.70, 127.09, 125.71, 108.65, and 25.80; HR-MS (ESI) m/z calculated for $C_{19}H_{14}O_3S$ ([M+H]$^+$): 323.0742; found: 323.0742.

• **3-Acetyl-4-hydroxy-5-((*E*)-3-phenylallylidene)thiophen-2 (5*H*)-one (12a).** Yellow solid; yield 63.1%; m.p. 138–139 °C; ^{1}H NMR (600 MHz, DMSO-d_6) δ: 7.64 (d, J = 7.2 Hz, 2H), 7.58 (d, J = 11.4 Hz, 1H), 7.39 (t, J = 7.2 Hz, 2H), 7.36 (d, J = 6.9 Hz, 1H), 7.35–7.28 (m, 1H), 6.98 (dd, J = 15.0, 11.6 Hz, 1H), and 2.45 (s, 3H). ^{13}C NMR (150 MHz, DMSO-d_6) δ: 196.63, 186.34, 183.88, 144.37, 136.10, 132.33, 130.32, 129.42, 128.34, 124.52, 110.07, and 27.09; HR-MS (ESI) m/z calculated for $C_{15}H_{12}O_3S$ ([M+H]$^+$): 273.0585; found: 273.0586.

2.3. Screening of antifungal activity in vitro

Each bioassay was performed in triplicate at (25 ± 1) °C. According to the mycelium growth rate method, **9a–9i, 10a–10g, 11a–11m**, and **12a** were screened for antifungal activities *in vitro* against four phytopathogenic fungi, *Valsa mali*, *Curvularia lunata*, *Fusarium graminearum*, and *Fusarium oxysporum* f. sp. *lycopersici*, at 50 μg·mL^{-1}. Activity results were estimated according to a percentage scale of 0–100. Detailed bioassay procedures for fungicidal activity have been described previously [20].

2.4. CoMFA calculation

The CoMFA method was used to investigate the QSAR of the synthesized compounds [21]. A total of 27 compounds were selected for the QSAR study, based on their chemical diversity and *C. lunata* inhibitory bioactivity. The 3D structures of 27 compounds were constructed using the default settings of SYBYL 7.3 software (Tripos™, Certara Inc., USA), and optimized with the steepest-descent algorithm to a convergence criterion of 0.005 kcal·mol^{-1} (1 kcal = 4184 J). The CoMFA descriptors, steric, and electrostatic field energies were calculated by the SYBYL default parameters: an sp^3 carbon probe atom with +1 charge, 2.0 Å rid points spacing, the energy cutoff of 30.0 kcal·mol^{-1}, and a minimum column filtering (σ) of 2.0 kcal·mol^{-1} [22–24].

3. Results and discussion

Compounds **4**, **11f**, **11i**, and **11n** were prepared in three steps, as previously described [20]. Compounds **6** and **8** were prepared by the esterification of the corresponding acid and alcohol in one step. The target compounds **9a–9i, 10a–10g**, **11a–11n**, and **12a** were obtained by condensation with intermediate **4**. Compound **11c′** was obtained by the reaction of **11c** with ethanol.

The structures of all of the target compounds were characterized by ^{1}H NMR, ^{13}C NMR, and HR-MS spectra. In addition, the crystal structure of **11c′** was determined by X-ray diffraction analyses. As shown in Fig. 2, the double bond formed by the dehydration of the aldol reaction product adopts a Z-configuration rather than an E-conformation.

3.1. Fungicidal activity

The preliminary determination of the inhibition rates of compounds **9a–9i, 10a–10g, 11a–11n**, and **12a** (50 μg·mL^{-1}) against four plant-pathogenic fungi (*V. mali*, *C. lunata*, *F. graminearum*, and *F. oxysporum* f. sp. *lycopersici*) is shown in Table 1. The data suggested that most of the target compounds displayed moderate to good fungicidal activities against all the tested fungi at a dose of 50 μg·mL^{-1}. In order to compare the potency of the synthetic chemicals, azoxystrobin, carbendazim, and fluopyram were used as positive controls.

To further explore the antifungal potential and structure–activity relationship (SAR), the compounds with inhibition rates greater than 70% at a concentration of 50 μg·mL^{-1} were used to further determine their regression equations and median effective concentration (EC_{50} values) toward the four tested fungi (Table 2).

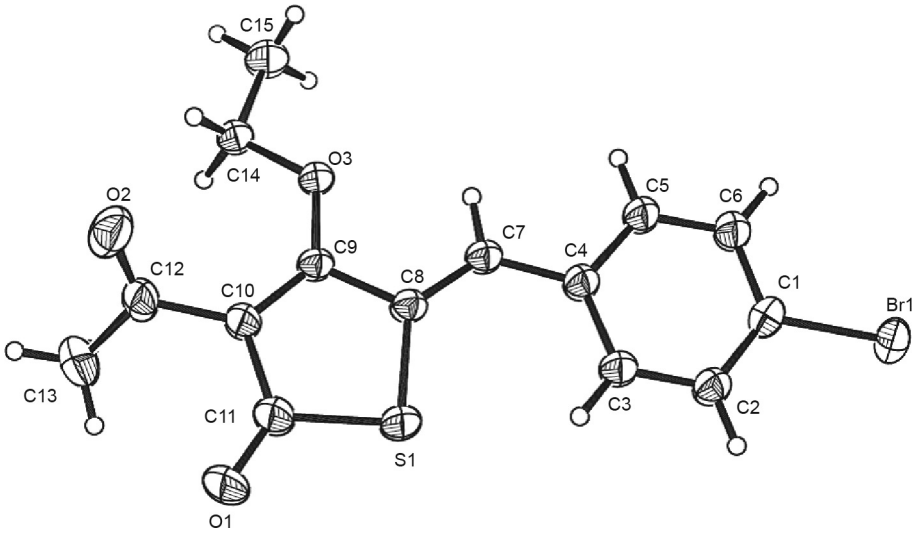

Fig. 2. X-ray single-crystal structure of **11c′**.

Table 1
Comparison of fungicidal activities of compounds **9a–9i**, **10a–10g**, **11a–11n**, and **12a** at a concentration of 50 μg·mL^{-1} against *V. mali*, *C. lunata*, *F. graminearum*, and *F. oxysporum* f. sp. *lycopersici*.

Compound	Fungicidal inhibition (%)			
	V. mali	*C. lunata*	*F. graminearum*	*F. oxysporum* f. sp. *lycopersici*
9a	42.7 ± 2.0	21.2 ± 4.1	19.3 ± 1.0	31.3 ± 0.0
9b	30.8 ± 0.9	35.3 ± 2.2	18.1 ± 3.8	37.8 ± 1.1
9c	26.9 ± 0.0	32.5 ± 0.0	40.2 ± 1.5	29.5 ± 0.7
9d	31.9 ± 3.7	10.6 ± 0.6	22.9 ± 1.3	32.4 ± 0.0
9e	25.2 ± 1.0	7.15 ± 1.1	21.7 ± 3.5	18.0 ± 3.6
9f	9.96 ± 0.0	47.5 ± 0.0	13.5 ± 0.0	10.0 ± 0.0
9g	26.6 ± 1.7	17.7 ± 1.9	18.5 ± 2.3	29.7 ± 0.0
9h	11.3 ± 4.2	5.25 ± 0.9	24.9 ± 5.4	15.3 ± 2.3
9i	18.8 ± 0.5	49.7 ± 0.0	40.2 ± 0.0	10.0 ± 0.0
10a	69.3 ± 0.5	38.7 ± 0.5	27.3 ± 0.6	68.4 ± 0.0
10b	70.2 ± 0.3	76.4 ± 0.0	41.4 ± 0.6	80.9 ± 0.6
10c	76.2 ± 0.5	75.0 ± 1.0	62.7 ± 1.0	82.7 ± 1.8
10d	57.0 ± 0.0	49.6 ± 2.3	51.8 ± 1.7	79.4 ± 0.8
10e	63.3 ± 0.0	32.9 ± 0.5	37.3 ± 0.0	61.7 ± 0.7
10f	3.60 ± 0.0	39.0 ± 0.0	2.42 ± 0.5	9.52 ± 0.7
10g	54.9 ± 0.0	54.3 ± 0.5	33.7 ± 1.0	41.6 ± 0.7
11a	84.5 ± 0.5	94.7 ± 0.0	72.8 ± 0.0	76.6 ± 0.7
11b	67.4 ± 0.0	96.8 ± 1.5	67.4 ± 1.6	85.9 ± 0.0
11c	93.0 ± 1.0	95.7 ± 0.0	64.1 ± 0.0	81.2 ± 1.3
11d	71.9 ± 1.0	86.3 ± 2.3	56.0 ± 0.9	66.0 ± 0.0
11e	72.6 ± 0.0	94.7 ± 0.9	64.3 ± 1.0	86.4 ± 0.0
11f	83.7 ± 0.3	92.5 ± 3.1	67.9 ± 0.9	80.2 ± 0.9
11g	90.8 ± 0.5	96.4 ± 1.0	65.9 ± 0.5	75.1 ± 0.7
11h	73.7 ± 0.0	96.4 ± 0.5	67.7 ± 2.0	85.9 ± 0.0
11i	83.8 ± 0.8	93.7 ± 1.8	69.1 ± 0.9	80.8 ± 0.9
11j	58.2 ± 2.0	52.6 ± 1.7	34.1 ± 2.0	57.0 ± 1.3
11k	86.7 ± 0.5	88.4 ± 1.7	57.1 ± 0.9	81.7 ± 0.5
11l	73.6 ± 2.0	82.1 ± 0.0	37.3 ± 3.7	70.1 ± 0.7
11m	37.9 ± 0.0	71.6 ± 0.5	32.6 ± 0.9	39.9 ± 0.7
12a	76.5 ± 3.5	90.4 ± 2.0	56.0 ± 0.0	69.2 ± 0.6
11n	90.4 ± 0.2	91.2 ± 0.8	72.8 ± 0.9	79.0 ± 0.9
Azoxystrobin	81.6 ± 0.0	54.7 ± 0.6	69.1 ± 0.0	79.8 ± 0.0
Fluopyram	6.0 ± 1.2	97.7 ± 0.0	97.8 ± 0.8	41.6 ± 0.7
Carbendazim	97.9 ± 0.4	100 ± 0.0	100 ± 0.9	58.0 ± 0.9

Table 1 shows that compounds **9a–9i** displayed weak inhibition (< 50% inhibition rate) against the target fungi. Compounds **10a** and **10d–10g** displayed different degrees of fungicidal activity, ranging from 5.25% to 82.7% inhibition against the tested fungi at a dose of 50 μg·mL^{-1}. It was interesting that compounds **10b**, **10c**, and **10d** were highly active (79.4%–82.7% inhibition at 50 μg·mL^{-1}) against *F. oxysporum* f. sp. *lycopersici*, while compounds **11a–11m** and **12a** exhibited moderate (35%–70%) to good activities (> 70% inhibition at 50 μg·mL^{-1}) against *V. mali*. In contrast (See Table 2), the EC_{50} values of compounds **11a, 11c**, **11f**, **11g**, **11i**, and **11k** ranged from 3.1 to 18.7 μg·mL^{-1}, while compound **11f** displayed a roughly similar level of antifungal activity

Table 2
EC_{50} values ($\mu g \cdot mL^{-1}$) of compounds **10b**, **10c**, **11a**–**11l**, and **12a** against *V. mali*, *C. lunata*, *F. graminearum*, and *F. oxysporum* f. sp. *lycopersici*.

Fungus	Compound	Toxicity regression equation	r^2	EC_{50} ($\mu g\ mL^{-1}$)	95% CI[a] of EC_{50}[b]
V. mali	**10b**	$y = 1.103x - 1.152$	0.87	11.1	6.73–21.6
	10c	$y = 0.846x - 0.816$	0.97	9.22	7.03–12.6
	11a	$y = 1.106x - 1.268$	0.90	14.0	8.20–31.4
	11b	$y = 1.054x - 1.107$	0.94	11.2	7.31–19.6
	11c	$y = 1.236x - 0.971$	0.96	6.11	5.04–7.45
	11d	$y = 0.884x - 1.094$	0.96	17.2	12.8–25.0
	11e	$y = 1.052x - 1.251$	0.98	15.5	12.1–20.8
	11f	$y = 1.417x - 0.688$	0.91	3.06	1.73–5.19
	11g	$y = 1.452x - 1.725$	0.89	15.4	9.05–35.1
	11h	$y = 0.906x - 0.942$	0.96	11.0	8.44–14.8
	11i	$y = 1.799x - 1.172$	0.99	4.48	3.86–5.22
	11j	$y = 1.010x - 1.003$	0.92	9.83	6.15–18.1
	11k	$y = 1.165x - 1.482$	0.98	18.7	14.8–24.9
	12a	$y = 1.116x - 1.077$	0.98	9.22	7.45–11.6
	Azoxystrobin	$y = 0.583x + 0.304$	0.92	0.30	0.034–0.87
	Fluopyram			> 50.0	
	Carbendazim	$y = 1.876x - 1.173$	0.91	4.22	1.13–14.4
C. lunata	**10b**	$y = 1.316x - 1.478$	0.96	13.3	9.48–20.2
	10c	$y = 1.616x - 1.842$	0.96	13.8	10.4–19.2
	11a	$y = 1.239x - 0.502$	0.97	2.54	2.04–3.10
	11b	$y = 1.384x - 0.520$	0.90	2.37	1.11–4.09
	11c	$y = 1.158x - 0.318$	0.98	1.88	1.46–2.35
	11d	$y = 1.292x - 0.940$	0.99	5.34	4.43–6.43
	11e	$y = 1.306x - 0.751$	0.99	3.76	3.11–4.52
	11f	$y = 1.602x - 1.476$	0.953	8.40	6.00–12.9
	11g	$y = 1.450x - 0.908$	0.98	4.23	3.56–5.01
	11h	$y = 1.113x - 0.225$	0.99	1.59	1.20–2.02
	11i	$y = 1.515x - 1.091$	0.98	5.30	4.43–6.31
	11k	$y = 0.799x - 0.245$	0.98	2.03	1.40–2.74
	11l	$y = 1.306x - 1.220$	0.98	8.59	7.13–10.5
	12a	$y = 1.302x - 0.729$	0.96	3.63	2.49–5.12
	Azoxystrobin	$y = 0.055x - 0.366$	0.90	6.70	4.61–11.8
	Fluopyram	$y = 0.891x + 0.669$	0.97	0.18	0.11–0.26
	Carbendazim	$y = 1.425x - 2.308$	0.84	41.7	19.8–48.6
F. graminearum	**10c**	$y = 1.265x - 1.646$	0.99	20.0	11.6–50.6
	11a	$y = 1.360x - 1.714$	0.99	18.2	11.4–36.9
	11b	$y = 1.006x - 1.185$	0.98	15.1	11.7–20.5
	11c	$y = 0.641x - 0.659$	0.92	10.7	7.49–16.5
	11f	$y = 0.873x - 0.635$	0.97	5.30	4.05–7.36
	11g	$y = 1.249x - 1.560$	0.97	17.8	14.3–23.0
	11h	$y = 0.905x - 0.874$	0.96	9.23	4.47–26.6
	11i	$y = 0.731x - 0.355$	0.98	3.10	2.15–4.25
	Azoxystrobin	$y = 0.467x - 0.632$	0.95	22.4	9.05–30.7
	Fluopyram	$y = 0.780x + 0.287$	0.93	0.43	0.093–1.11
	Carbendazim	$y = 1.703x + 0.641$	0.95	0.42	0.17–0.99
F. oxysporum f. sp. *lycopersici*	**10b**	$y = 1.174x - 1.050$	0.98	7.84	6.41–9.72
	10c	$y = 1.220x - 0.892$	0.95	5.39	4.33–6.61
	11a	$y = 1.055x - 1.089$	0.99	10.8	8.57–14.0
	11b	$y = 1.008x - 0.877$	0.95	7.41	5.90–9.48
	11c	$y = 1.160x - 0.758$	0.83	4.50	2.23–8.56
	11e	$y = 1.416x - 1.475$	0.98	11.0	9.20–13.4
	11f	$y = 1.782x - 1.780$	0.97	10.0	8.42–12.9
	11g	$y = 1.064x - 1.093$	0.99	10.6	8.48–13.7
	11h	$y = 1.236x - 0.911$	0.99	5.46	4.50–6.63
	11i	$y = 1.643x - 1.467$	0.97	7.80	6.59–9.47
	11k	$y = 1.264x - 1.129$	0.99	7.82	6.47–9.56
	11l	$y = 1.172x - 1.427$	0.99	16.5	13.1–21.6
	12a	$y = 1.188x - 1.344$	0.96	13.5	10.9–17.3
	Azoxystrobin	$y = 1.086x - 0.693$	0.98	4.30	4.35–4.39
	Fluopyram			> 50.0	
	Carbendazim	$y = 1.885x + 6.723$	0.907	0.12	0.096–0.36

[a] 95% CI: confidence intervals at 95% probability; [b] average of three replicates.

to that of carbendazim (EC_{50} = 4.2 $\mu g \cdot mL^{-1}$) against *V. mali*, which was superior to that of fluopyram (EC_{50} > 50 $\mu g \cdot mL^{-1}$) and ten-fold greater than that of azoxystrobin (EC_{50} = 0.3 $\mu g \cdot mL^{-1}$). In regard to *C. lunata*, the EC_{50} of compounds **11a**–**11k** and **12a** ranged from 1.9 to 8.96 $\mu g \cdot mL^{-1}$, with some of these compounds exhibiting more fungicidal activity than the positive controls azoxystrobin (EC_{50} = 6.7 $\mu g \cdot mL^{-1}$) and carbendazim (EC_{50} = 41.2 $\mu g \cdot mL^{-1}$); these values can be compared with the EC_{50} of fluopyram, which is 0.18 $\mu g \cdot mL^{-1}$. It was interesting that compound **11j** had low inhibition against *C. lunata*. In regard to *F. graminearum*, compounds **11a**–**11m** and **12a** had low (< 35% inhibition) to moderate potencies (35%–70% inhibition) at 50 $\mu g \cdot mL^{-1}$; compound **11i** exhibited the highest fungicidal activity (EC_{50} = 3.1 $\mu g \cdot mL^{-1}$), which was 7.2- and 7.4-fold greater than those of fluopyram (EC_{50} = 0.43 $\mu g \cdot mL^{-1}$) and carbendazim (EC_{50} = 0.42 $\mu g \cdot mL^{-1}$), respectively. In regard to *F. oxysporum* f. sp. *lycopersici*, compounds **11a**–**11m** and **12a**

inhibited *F. oxysporum* f. sp. *lycopersici* with an inhibition higher than 50% with the exception of compound **11m**, which had an EC_{50} of 4.5–16.5 $\mu g \cdot mL^{-1}$; compound **11c** displayed the highest fungicidal activity. The EC_{50} values of compound **11c,** azoxystrobin, and carbendazim were 4.5, 4.3, and 0.123 $\mu g \cdot mL^{-1}$, respectively. The results showed that compound **11c** exhibited a roughly similar level of antifungal activity to azoxystrobin and a level that was 37-fold greater than that of carbendazim.

3.2. CoMFA studies

3D-QSAR is widely used in the drug and pesticide discovery process to describe the SARs of compounds. To investigate the substituent effect on *C. lunata* inhibitory activity, a CoMFA model for the 28 compounds was developed. The conventional coefficient r^2 of the CoMFA model was 0.9816, the cross-validated coefficient q^2 was 0.8060, and the predicted noncross-validated coefficient r^2(pred) was 0.9693. The plots of the predicted inhibitory activities against *C. lunata* versus the experimental values are shown in Fig. 3(a), and the alignment result of the 22 training set compounds is shown in Fig. 3(b). The steric field contour maps are shown in green and yellow (Fig. 3(c)). The yellow polyhedra shows that bulky substituents at these sites were detrimental to activity. For example, when an ester group or alkoxycarbonyl was introduced, compounds **9a**–**9i** showed lower activity than their parent compound **11n**; the same trend can be found in compounds **10a**–**10g**. In comparison, the green polyhedra indicates that small substituents are favorable to activity. The electrostatic contour maps are shown in Fig. 3(d), where the blue contours indicate that positive charges in these areas will increase inhibitory activity against *C. lunata*. For example, compounds with a halogen atom at the 4-position of the benzene ring displayed higher activity than **11n**; thus, introducing a bromine atom to **11n** would significantly increase its bioactivity (i.e., **11c** > **11n**, **11f** > **11n**, and **11i** > **11n**). The red contours indicate that negative charges in these areas are unfavorable to activity, which supported the finding that compound **11j**, which contains cyano groups, would display decreased activity (i.e., **11n** > **11j**).

4. Conclusions

In summary, a series of 3-acylthiotetronic acid derivatives **9a**–**9i**, **10a**–**10 g**, **11a**–**11 m**, and **12a** were designed and synthesized in the present study. The biological assay results indicated that most of the target compounds possessed *in vitro* antifungal activities toward the fungal pathogens *V. mali*, *C. lunata*, *F. graminearum*, and *F. oxysporum* f. sp. *lycopersici*. Compounds **11c** and **11i** displayed broad-spectrum fungicidal activity with respective EC_{50} values of 1.9–10.7 and 3.1–7.8 $\mu g \cdot mL^{-1}$ against the tested four fungal species. The results of the bioassays and QSAR studies indicated that bulky substituents at *para*-position of benzene ring could significantly decrease the antifungal activities of the target compounds. It was noteworthy that the introduction of a halogen atom at the benzene ring of benzylidene could improve the activity against the tested fungi. Further studies on the structural optimization and biological evaluation of the compounds are in progress.

Acknowledgements

This work was financially supported in part by the National Natural Science Foundation of China (31901906), the Opening Project of Shanghai Key Laboratory of Chemical Biology, the Natural Science Foundation of Anhui Province, China (1808085QC71), the Natural Science Foundation of Anhui Education Department (KJ2016A834), and the US Department of Agriculture (USDA: HAW5032-R).

Compliance with ethics guidelines

Pei Lv, Yiliang Chen, Dawei Wang, Xiangwei Wu, Qing X. Li, and Rimao Hua declare that they have no conflict of interest or financial conflicts to disclose.

Appendix A. Supplementary data

Supplementary data to this article can be found online at https://doi.org/10.1016/j.eng.2019.10.016.

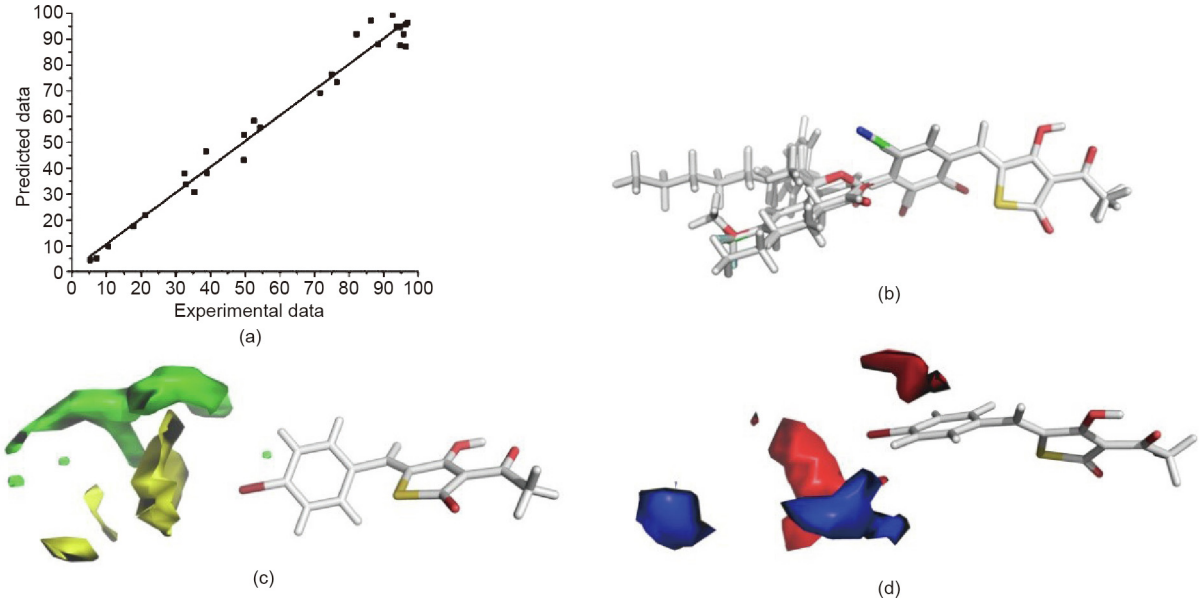

Fig. 3. CoMFA calculations. (a) CoMFA model predicted values versus experimental inhibitory values. (b) Structural alignment of 22 training set compounds. (c) Contour map of steric contribution, where compound **11c** is shown inside the field. The yellow polyhedra indicates that sterically bulky substituents are detrimental to activity, while the green polyhedra shows that sterically bulkier substituents are favorable to activity. (d) Contour map of electrostatic contribution, where compound **11c** is shown inside the field. Blue contours indicate that positive charges in these areas will increase the activity; red contours indicate that negative charges in these areas will decrease the activity.

References

[1] Pennisi E. Armed and dangerous. Science 2010;327(5967):804–5.
[2] Anderson PK, Cunningham AA, Patel NG, Morales FJ, Epstein PR, Daszak P. Emerging infectious diseases of plants: pathogen pollution, climate change and agrotechnology drivers. Trends Ecol Evol 2004;19(10):535–44.
[3] Fisher MC, Henk DA, Briggs CJ, Brownstein JS, Madoff LC, McCraw SL, et al. Emerging fungal threats to animal, plant and ecosystem health. Nature 2012;484(7393):186–94.
[4] Sparks TC, Lorsbach BA. Perspectives on the agrochemical industry and agrochemical discovery. Pest Manag Sci 2017;73(4):672–7.
[5] Zhang YJ, Yu JJ, Zhang YN, Zhang X, Cheng CJ, Wang JX, et al. Effect of carbendazim resistance on trichothecene production and aggressiveness of Fusarium graminearum. Mol Plant Microbe Interact 2009;22(9):1143–50.
[6] Dijksterhuis J, Van Doorn T, Samson R, Postma J. Effects of seven fungicides on non-target aquatic fungi. Water Air Soil Pollut 2011;222(1–4):421–5.
[7] Belgers JDM, Aalderink GH, Van den Brink PJ. Effects of four fungicides on nine non-target submersed macrophytes. Ecotoxicol Environ Saf 2009;72 (2):579–84.
[8] Jenni S, Leibundgut M, Maier T, Ban N. Architecture of a fungal fatty acid synthase at 5 Å resolution. Science 2006;311(5765):1263–7.
[9] Wakil SJ, Stoops JK, Joshi VC. Fatty acid synthesis and its regulation. Annu Rev Biochem 1983;52(1):537–79.
[10] Schweizer E, Hofmann J. Microbial type I fatty acid synthases (FAS): major players in a network of cellular FAS systems. Microbiol Mol Biol Rev 2004;68 (3):501–17.
[11] Kremer L, Douglas JD, Baulard AR, Morehouse C, Guy MR, Alland D, et al. Thiolactomycin and related analogues as novel anti-mycobacterial agents targeting KasA and KasB condensing enzymes in Mycobacterium tuberculosis. J Biol Chem 2000;275(22):16857–64.
[12] White SW, Zheng J, Zhang YM, Rock CO. The structural biology of type II fatty acid biosynthesis. Annu Rev Biochem 2005;74(1):791–831.
[13] Nishida I, Kawaguchi A, Yamada M. Effect of thiolactomycin on the individual enzymes of the fatty acid synthase system in *Escherichia coli*. J Biochem 1986;99(5):1447–54.
[14] Furukawa H, Tsay JT, Jackowski S, Takamura Y, Rock CO. Thiolactomycin resistance in *Escherichia coli* is associated with the multidrug resistance efflux pump encoded by emrAB. J Bacteriol 1993;175(12):3723–9.
[15] Sakya SM, Suarez-Contreras M, Dirlam JP, O'Connell TN, Hayashi SF, Santoro SL, et al. Synthesis and structure–activity relationships of thiotetronic acid analogues of thiolactomycin. Bioorg Med Chem Lett 2001;11(20): 2751–4.
[16] Jones AL, Herbert D, Rutter AJ, Dancer JE, Harwood JL. Novel inhibitors of the condensing enzymes of the type II fatty acid synthase of pea (*Pisum sativum*). Biochem J 2000;347(Pt 1):205–9.
[17] Jones SM, Urch JE, Brun R, Harwood JL, Berry C, Gilbert IH. Analogues of thiolactomycin as potential anti-malarial and anti-trypanosomal agents. Bioorg Med Chem 2004;12(4):683–92.
[18] Jones SM, Urch JE, Kaiser M, Brun R, Harwood JL, Berry C, et al. Analogues of thiolactomycin as potential antimalarial agents. J Med Chem 2005;48 (19):5932–41.
[19] Nayyar A, Jain R. Recent advances in new structural classes of anti-tuberculosis agents. Curr Med Chem 2005;12(16):1873–86.
[20] Lv P, Chen Y, Zhao Z, Shi T, Wu X, Xue J, et al. Design, synthesis, and antifungal activities of 3-acyl thiotetronic acid derivatives: new fatty acid synthase inhibitors. J Agric Food Chem 2018;66(4):1023–32.
[21] Cherkasov A, Muratov EN, Fourches D, Varnek A, Baskin II, Cronin M, et al. QSAR modeling: where have you been? Where are you going to? J Med Chem 2014;57(12):4977–5010.
[22] Wang DW, Lin HY, He B, Wu FX, Chen T, Chen Q, et al. An efficient one-pot synthesis of 2-(aryloxyacetyl)cyclohexane-1,3-diones as herbicidal 4-hydroxyphenylpyruvate dioxygenase inhibitors. J Agric Food Chem 2016;64 (47):8986–93.
[23] Wang DW, Lin HY, Cao RJ, Chen T, Wu FX, Hao GF, et al. Synthesis and herbicidal activity of triketone–quinoline hybrids as novel 4-hydroxyphenylpyruvate dioxygenase inhibitors. J Agric Food Chem 2015;63 (23):5587–96.
[24] Wang DW, Li Q, Wen K, Ismail I, Liu DD, Niu CW, et al. Synthesis and herbicidal activity of pyrido[2,3-*d*]pyrimidine-2,4-dione-benzoxazinone hybrids as protoporphyrinogen oxidase inhibitors. J Agric Food Chem 2017;65 (26):5278–86.